SURFACE BURNOFF DURING BULK OXIDATION OF GRAPHITE

F. B. Growcock, M. Eto, J. Heiser, III and C. S. Sastre

Graphite specimens have been oxidized in air, water vapor and water vapor with added hydrogen. Density profiles of the oxidized specimens are inconsistent with the expected burnoff behavior. The results are explained in terms of a bimodal pore structure wherein the density of micropore-macropore interconnections within the solid is low, contrary to the widely-held view. Reaction near the surface, as well as throughout the bulk, of specimens presumably oxidized in the chemical reaction control regime can lead to erroneous assessment of the kinetics.

Diffusion, graphite, kinetics, oxidation, structure.

Introduction

The structural integrity of nuclear graphites has been a hotly debated topic, particularly with regard to long-term corrosive effects of hot gases. The use of high-purity, low permeability synthetic graphites in nuclear reactors such as the High Temperature Gas-Cooled Reactor (HTGR) has prompted many workers to characterize these materials extensively, so that much progress has been made toward understanding the gasification of graphite by gaseous impurities in the coolant. The roles of gaseous mass transport [1-3], catalysis [4], and structural changes [5,6] accompanying oxidation are well appreciated. Reaction rate modeling has become sophisticated enough to include these processes, as well as deviations from isothermality, equimolar diffusion and first order intrinsic chemical kinetics expressions [7]. Even with the aid of such models, however, extrapolation of laboratory-derived reaction rate data to reactor conditions can be fraught with pitfalls. One such pitfall, which is examined in this paper, is the presumption that gasification of small graphite specimens at low temperatures is under chemical reaction control.

Experimental Techniques

Axial cylindrical specimens 19 mm ø x 38 mm and 38 mm ø x 76 mm were machined (with a precision lathe to a tolerance of 0.01 mm) from the midlengths of logs of H451 graphite (Great Lakes Carbon Corp.) and PGX graphite (Union Carbide Corp.), ultrasonically cleaned in absolute methanol and dried at 75°C for several hours. These were oxidized in particulate-free dried air at 450 to 550°C and H_2O in He at 650 to 850°C. The H_2O mixtures were made by passing high-purity He through a bubbler maintained at 18°C to give 2000 Pa H_2O or blending that mixture with He and high-purity H_2 to give a final mixture containing 170 Pa H_2O and 1700 Pa H_2 in He. All experiments were conducted at atmospheric pressure using a flow rate that produced <1% conversion of the oxidant.

The smaller specimens were simply laid on the bottom of a quartz combustion tube and oxidized in that position. Two H451 specimens were encased in tight crucibles of the same material, "cocoons", so that the inner walls of the "cocoons" contacted the specimens everywhere. The larger specimens were suspended in the gas stream and the cylinder faces were sealed off. Gas chromatography was used to continuously monitor the reaction products CO and CO_2.

Density profiles were measured with a precision lathe until the specimens fractured. Control specimens were also profiled. Narrow regions of abnormal density were occasionally observed, as was the case for the oxidized specimens, but no trends in density were noticed.

Results and Discussion

The effect of temperature on reaction rate of the small H451 specimens with air and H_2O indicates that in-pore diffusion does not limit the reactions below 550°C and 850°C, respectively. In-pore diffusion begins to have a noticeable effect on PGX specimens oxidized in air above 600°C and in H_2O above 850°C. A typical density profile of a specimen presumably oxidized in the chemical reaction control regime is plotted in Figure 1 in the form local burnoff versus depth. The ordinate scale on the right gives the total burnoff of the residual core at each step of the machining process. Near the surface the burnoff profile is sharp and has a shape expected for a reaction limited by in-pore diffusion. However, the burnoff does not approach zero in the interior. The constant burnoff level in the interior is that expected for chemical reaction control.

All specimens tested behaved as indicated for the specimen in Figure 1. Similar behavior has been observed before in our group [8] and elsewhere [9]. It is conceivable that in-pore diffusion-limited oxidation could manifest itself in the manner described. Since the cylinder faces were not masked, oxidation in these regions would contribute a constant total burnoff to the profile, and perhaps a little more around the edges. However, since the external surface area of the faces is only 1/4 that of the cylinder wall, the mass loss contribution from the faces to the bulk burnoff is less than 10% of the measured bulk burnoff in our experiments. This was verified by oxidizing two 12.7 mm ø x 76 mm PGX cylinders in air, carefully removing 15 mm from each end and measuring the density profiles as before. Burnoff profiles similar in shape to that in Figure 1 were obtained.

This phenomenon is being investigated in greater detail. First, it should be noted that no particulate matter was recovered after the experiments and, within tolerance limits, no change in the external dimensions of the specimens was noticeable. Second, no measurable temperature gradient across the specimen diameters was observed using an internal thin, shielded thermocouple. Third, no other simultaneous (parallel) chemical reaction, including inhibition by reaction products, can account for the observed burnoff profiles. Inhibition by products CO/CO_2 or CO/H_2 cannot lead to a flat profile in the interior of a specimen. This was, nevertheless, verified in the following manner. If inhibition by reaction products can produce the phenomenon, the burnoff profile should be quite different in the case where reactant and product gases have to diffuse through a barrier at the graphite surface. A "cocoon" experiment was run with H451 graphite in air. The burnoff profile shown in Figure 2 for one of these experiments is similar to the previous profiles, indicating that the effect of the reaction products is too small to produce much deviation from a flat profile.

Another possible explanation is that the density of active sites on the surfaces of the unoxidized specimens is higher than in the interior. Active surface area profiles of H451 and PGX graphite show little difference in the active surface area between the outer and inner regions of the specimens, in agreement with specific (B.E.T.) surface area measurements (see also reference [9]).

Walker, et al. [9] speculated that the micropores in their material (pure carbon rods) might be responsible for the burnoff near the surface. However, it was believed at that time, and still is, that the micropores are so interconnected to macropores that their effective lengths are too short to cause the observed behavior. To determine how the structure of graphite could lead to the observed burnoff behavior, its pore network was scrutinized. Photomicrographs of highly polished, gold-sputtered H451 specimens were examined. Pores as small as 0.2 μm could be measured. The distribution of pores in the size range above 8 μm over an area of 0.35 cm^2 is shown in Figure 3. The pore size distribution between 10 Å and 10,000 Å has been measured previously [10]. The pores can be divided into three groups with average pore diameters of 40 Å, 0.20 μm and 20 μm. The micropores occupy a void volume of ≈ 0.04 (40 Å pores), whereas the macropores (0.20 μm and 20 μm pores) occupy a volume of ≈ 0.14. Thus, the number of micropores per unit volume is several orders of magnitude greater than that of the macropores, and the average distance between macropores is large enough (≈ 1 μm and 100 μm for the small and large macropores, respectively) that the concentration of reactant gas in the micropores can be large for a significant distance into the specimen. A schematic of the observed oxidation profile of graphite is shown in Figure 4. The graphite furnishes two paths for the reactant gas: a surface network, $\Sigma_{surface}$, consisting of micropores open at the surface and a bulk network, Σ_{bulk}, consisting of the entire assembly of pores. Since the accessible active surface area per unit volume of specimen is much greater in $\Sigma_{surface}$ than in Σ_{bulk}, reactivity in the surface region is higher than in the bulk.

If the open micropores at the surface are responsible for the observed burnoff phenomenon, it should be possible to obtain some information about their average size. Effective diffusion coefficients were calculated from measured surface burnoffs (total burnoff minus bulk burnoff) and diffusion lengths using an expression after Dodson [11,12]. The diffusion length (the depth at which the reactant concentration is e⁻¹ lower than its concentration in the gas stream) can be obtained from the expression

$$C_R/C_{R_0} = (B-B_b)/(B_0-B_b) = \exp(-x/L)$$

where B is the fractional mass loss at a depth x into the specimen, B_b is the average fractional mass loss attributed to bulk burnoff, B_0 is the mass loss at the surface, C_R and C_{R_0} are the oxidant concentrations at x and at the surface and L is the diffusion length. L, obtained from the slopes of the density profiles, varied from 0.07 to 0.30 mm. The effective diffusion coefficient at the surface can be expressed by $D_{eff} = D_{gas}/\tau$,

where D_{12} is the free binary gas diffusion coefficient [13]. Values of m_s are plotted in Figure 5 for several levels of surface burnoff under various conditions.

Diffusion in the micropores of H451 graphite is controlled by Knudsen flow, since they average only 20 Å in radius. Effective (Knudsen) diffusion coefficients calculated for an average pore size of 20 Å using the dusty gas model [3] are 1.68×10^{-5} cm^2/sec for O_2 at 500°C and 2.64×10^{-5} cm^2/sec for H_2O at 800°C. Comparison of these crudely estimated values with the m_s values in Figure 5 suggests that Knudsen diffusion in the micropores is the predominant transport mechanism during the first stages of the oxidation.

Also plotted in Figure 5 are overall effective diffusion coefficients for PGX graphite oxidized in the diffusion-limited temperature regime; here $D_{eff} = mD_{12}$. The effective diffusion coefficient in H451 graphite is assumed to be ~ 0.01 D_{12} [14]; that of PGX is probably similar. This value was not obtained under reaction conditions; thus, small pores of relatively long length, as well as blind pores, do not contribute to the measured diffusion coefficient. The effective diffusion coefficients measured here under reaction conditions indicate that during the early stages of oxidation the effective diffusion coefficient is two orders of magnitude lower than the assumed value. Similar observations have been made by other workers [15]. This result suggests that the micropores significantly affect the kinetics of specimens oxidized in the diffusion-limited regime as well as in the chemical reaction control regime.

Conclusions

Oxidation of graphite specimens in the chemical reaction control regime can lead to some burnoff near the surface, which has been interpreted as oxidation in a relatively long micropore network. The reaction kinetics of large specimens oxidized in the chemical reaction control regime may be affected very little by this phenomenon, but the kinetics of small specimens will be affected significantly. This phenomenon may also be important at higher temperatures, where mass transport influences the overall reaction rate.

Acknowledgements

This work was performed under the auspices of the United States Nuclear Regulatory Commission. The photomicrography was done by R. Sabatini of the Metallurgy and Materials Sciences Division.

References

1. Aris, R., The Mathematical Theory of Diffusion and Reaction in Permeable Catalysts, Vol. 1. Clarendon Press, Oxford (1975).
2. Carberry, J.J., Chemical and Catalytic Reaction. McGraw-Hill, New York (1976).
3. Jackson, R., Transport in Porous Catalysts. Elsevier, New York (1976).
4. Walker, P.L., Jr., Shelef, M. and Anderson, P.A., Chemistry and Physics of Carbon (Edited by P.L. Walker, Jr.), Vol. 4, p. 287. Marcel Dekker, New York (1968).
5. Petersen, E.E., AIChE J. 3, 443 (1957).
6. Schechter, R.S. and Gidley, J.L., AIChE J. 15, 339 (1969).
7. Szekely, J., Evans, J.W. and Sohn, H.Y., Gas-Solid Reactions. Academic Press, New York (1976).
8. Romano, A.J. and Chow, J.G.Y., "Proceedings of the Topical Meeting on Thermal Reactor Safety, Sun Valley, Idaho, American Nuclear Society (1977).
9. Walker, P.L., Jr., Rusinko, F., Jr. and Austin, L.G., Advan. Catalysis 11, 133 (1959).
10. Yang, R.T. and Liu, R-T., Ind. Eng. Chem. Proc. Des. Dev. 18, 245 (1979).
11. Dodson, M.H., UKAEA Development and Engineering Report 148 (CA), (1960).
12. Burnette, P.D., Velasquez, C., Hightower, G. and Koyama, K., 13th Biennial Carbon Conference, Irvine, California, American Carbon Society (1977).
13. Reid, R.C. and Sherwood, T.K., The Properties of Gases and Liquids. McGraw-Hill, New York (1958).
14. Peroomian, M.B., Barsell, A.W. and Sanger, J.C., General Atomic Report, GA-A12493 (1974).
15. HTGR Fuels and Core Development Program Quarterly Progress Report Ending February 28, 1978, General Atomic Company, GA-A14363 (1978).

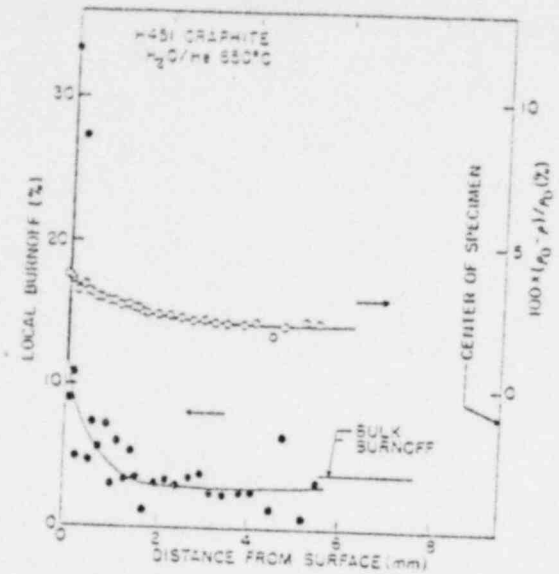

Figure 1. Burnoff profile of H451 graphite oxidized at 850°C in 2% H_2O/He to 4.10% burnoff.

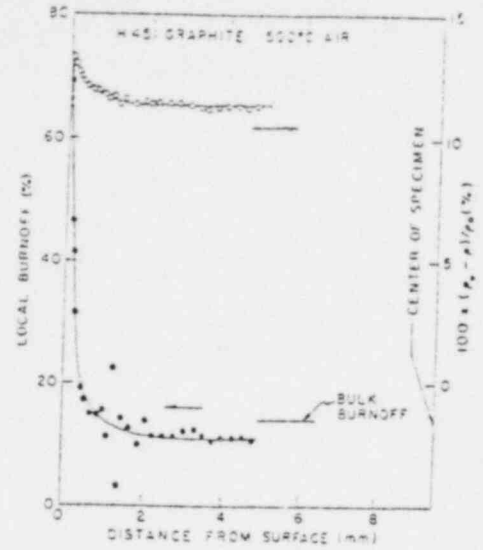

Figure 2. Burnoff profile of H451 graphite oxidized in a cocoon of the same material at 500°C in air to 14.1% burnoff.

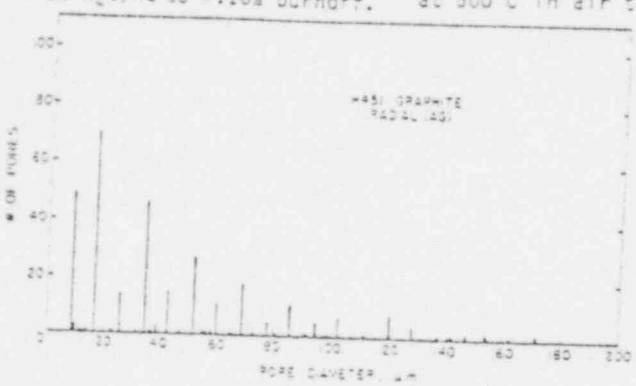

Figure 3. Density distribution of pores > 8 μm in H451 graphite

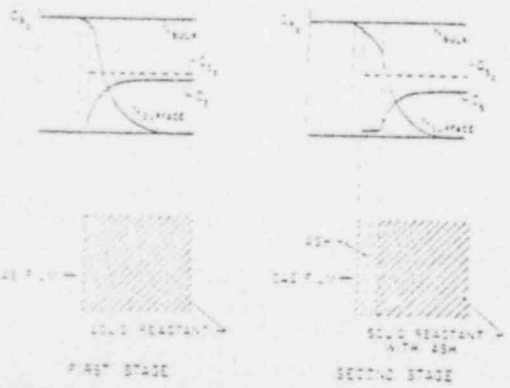

Figure 4. Schematic diagram of reactant concentration profiles in the gasification of graphite.

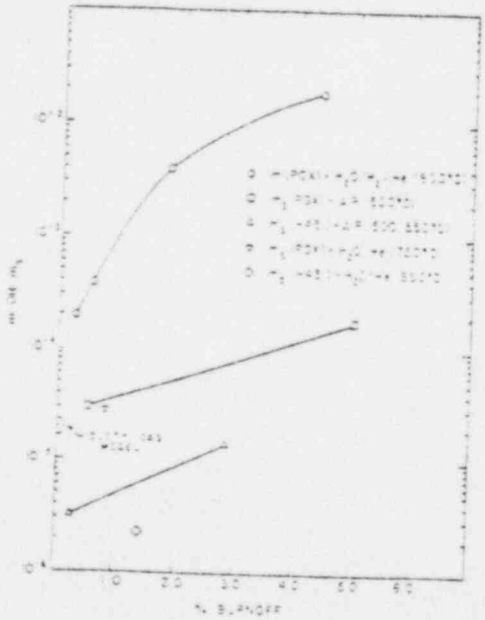

Figure 5. Dependence of the effective diffusion coefficient on burnoff under various conditions.